Evapotranspiration in hydrological models under rising CO2: a jump into the unknown

Thibault Lemaitre-Basset, Ludovic Oudin, Guillaume Thirel

Climatic Change (2022) 172: 36
https://doi.org/10.1007/s10584-022-03384-1

Evapotranspiration in hydrological models under rising CO_2: a jump into the unknown

Thibault Lemaitre-Basset[1,2] · **Ludovic Oudin**[1] · **Guillaume Thirel**[2]

Received: 9 November 2021 / Accepted: 28 May 2022 / Published online: 20 June 2022

Abstract

Many hydrological models use the concept of potential evapotranspiration (PE) to simulate actual evapotranspiration (AE). PE formulations often neglect the effect of carbon dioxide (CO_2), which challenges their relevance in a context of climate change and rapid changes in CO_2 atmospheric concentrations. In this work, we implement three options from the literature to take into account the effect of CO_2 on stomatal resistance in the well-known Penman–Monteith PE formulation. We assess their impact on future runoff using the Budyko framework over France. On the basis of an ensemble of Euro-Cordex climate projections using the RCP 4.5 and RCP 8.5 scenarios, we show that taking into account CO_2 in PE formulations largely reduces PE values but also limits projections of runoff decrease, especially under an emissive scenario, namely, the RCP 8.5, whereas the classic Penman–Monteith formulation yields decreasing runoff projections over most of France, taking into account CO_2 yields more contrasting results. Runoff increase becomes likely in the north of France, which is an energy-limited area, with different levels of runoff response produced by the three tested formulations. The results highlight the sensitivity of hydrological projections to the processes represented in the PE formulation.

Keywords Potential evapotranspiration · Climate projections · Runoff projections · CO_2 effect

Key points
We used three options for taking into account CO_2 in the Penman–Monteith potential evapotranspiration formulation.
Potential evapotranspiration is decreased when using CO_2 in the formulation but this decrease depends on how CO_2 is used in the formulation.
In energy-limited areas, future simulated runoff shows higher values when CO_2 is used.

✉ Thibault Lemaitre-Basset
thibault.lemaitre@inrae.fr

[1] UMR 7619 METIS, Sorbonne Université, CNRS, EPHE, Case 105, 4 place Jussieu, 75005 Paris, France

[2] Université Paris-Saclay, INRAE, HYCAR Research Unit, Antony, France

1 Introduction

1.1 Surface–atmosphere interactions in hydrological models

Hydrological models are widely used to assess the regional impacts of climate change on the components of the hydrological cycle (Roudier et al. 2016; Hakala et al. 2019). Most of these hydrological models use conceptual offline (i.e., uncoupled) representations of the soil–vegetation–atmosphere dynamics, through the concept of potential evapotranspiration. The term "evapotranspiration" incorporates two different fluxes: water evaporation from open water surfaces (abiotic process) and plant transpiration resulting from photosynthesis activity (biotic process). Climate change affects evapotranspiration due to increases in air temperature, radiation, and the maximum amount of water vapor in the air. Hereafter, we will focus on the role of carbon dioxide (CO_2) in the representation of the evapotranspiration process for hydrological simulation.

The use of potential evapotranspiration (PE) as an estimation of the atmospheric evaporative demand implicitly assumes rather stationary environmental conditions, e.g., in terms of land use and plant physiology, which is questionable in the current evolving climate and vegetation conditions (e.g., Yin et al. 2017; Bosmans et al. 2017). Such an assumption might become even more problematic when assessing the water cycle under future changing conditions, which will present drastic modifications in climate and land use. Differences between projected future AE rates and water resources obtained from conceptual hydrological models and from more integrative general circulation models were attributed by some authors to the use of a reference PE formulation with fixed parameters (e.g., albedo, constant of the stomatal and aerodynamic resistances), precluding the possibility of representing changes in vegetation processes (Kumar et al. 2016; Yang et al. 2019). This suggests that the conventional use of "reference" PE needs to be revised in order to improve the realism of hydroclimatic projections (Milly and Dunne 2016).

Adapting the PE formulations is a possible way of taking into account surface–atmosphere interactions in a simplified way. These adaptations include changes in albedo and in stomatal and aerodynamic resistances, which are sensitive to climate and to land use (Bosmans et al. 2017). Among these adaptations, integrating the role of rising atmospheric carbon dioxide (CO_2), in particular, has been investigated in the past decade (e.g., Butcher et al. 2014; Islam et al. 2012; Cheng et al. 2014).

1.2 The role of carbon dioxide in plant water use and how it is parameterized in hydrological models

Plant stomata enable gaseous exchange with the atmosphere for respiration and photosynthesis and they regulate AE. It is well-known that under higher atmospheric CO_2 concentrations, the gaseous exchange of plants is altered (Allen 1990, 1991). The stomatal opening regulates the carbon gain used for photosynthesis and consequently for vegetation growth. Environmental experiments have demonstrated that elevated atmospheric CO_2 concentrations reduce stomatal opening for transpiration in plants (Allen 1990), resulting in a lower water loss through stomata. However, terrestrial vegetation remains an important carbon sink and the feedback from CO_2 fertilization plays a role in PE. An elevated atmospheric CO_2 concentration promotes plant growth and

induces a larger leaf surface for AE (Le Quéré et al. 2015). It remains under discussion whether the resultant CO_2-induced lower transpiration may be canceled by higher crop transpiration through CO_2-induced increased biomass (Wada et al. 2013). Both effects have been demonstrated and quantified in controlled environments, but transposition of these results under field conditions and over longer time periods is still debated (Rosenberg et al. 1989; Bunce 2004; Cheng et al. 2014). At the global scale, Gedney et al. (2006) found that elevated atmospheric CO_2 concentrations and subsequent stomatal closure were partly responsible for the general upward trend in continental-scale river runoff during the past century, which is confirmed by simulations of several climate models predicting increased runoff in some regions (Yang et al. 2019). Overall, uncertainty about how vegetation responds to future increases in CO_2 and the consequences for water flow is a key question under investigation (Gerten et al. 2014). As the effect of CO_2 on reduced stomatal opening and increase biomass differs across biomes, human-induced or natural vegetation changes are also likely to play a significant role in AE trends (Inauen et al. 2013; Cheng et al. 2014), and crop fields (Bosmans et al. 2017). Offline impact models such as conceptual hydrological models differ largely in the way they deal with the effects of elevated atmospheric CO_2 concentrations on evapotranspiration. Most studies showed a strong increase in AE as a response to increased air temperature and vapor pressure deficit (Scheff and Frierson 2014; Naumann et al. 2018). However, some studies found that taking into account the active role of vegetation limits the increase in AE (e.g., Ma and Zhang 2022). This results in a general decrease in soil moisture and river flow, particularly in energy-limited regions (Chiew et al. 2009; Addor et al. 2014; Forzieri et al. 2014; Donnelly et al. 2017). Different results were found in studies where the authors took into account atmospheric CO_2 concentrations (Kruijt et al. 2008; Guillod et al. 2018), suggesting that the inclusion of CO_2 and a more explicit representation of vegetation dynamics can fundamentally change the drought response to climate change (Prudhomme et al. 2014; Pan et al. 2015; Yang et al. 2019).

The most straightforward way to take into account elevated CO_2 concentrations in hydrological models is to consider the relationship between changes in CO_2 concentrations and changes in stomatal resistance with the Penman–Monteith PE formulation. Based on experimental results, several equations were proposed and applied in impact studies (Allen 1990; Stockle et al. 1992; Yang et al. 2019) but few guidelines exist on the choice of the relationship and its consequences on modeling results.

1.3 Scope of the study

This study aims at quantifying the difference between several existing schemes to account for elevated atmospheric CO_2 concentrations in PE estimations and subsequent runoff estimations. On the basis of previous findings, we consider in our analysis the impact of CO_2 concentrations on stomatal resistance by applying three existing equations based on the modification of the stomatal resistance r_s in the Penman–Monteith formulation. This study could help to improve PE representation in rainfall–runoff models for climate impact studies and to better quantify corresponding uncertainties. We perform this analysis on the French metropolitan territory, which encompasses both water-limited (in the southern part) and energy-limited (in the northern part) regions, thus potentially showing a contrasting effect of PE estimates on runoff estimation.

2 Materials and methods

2.1 Climate model projections

The past range of atmospheric CO_2 concentration is not sufficient to yield to important changes in r_s, and therefore, working on past observations does not make it possible to decipher the effect of CO_2 on PE amounts. Consequently, we chose to work on future climate conditions using the outputs of eight CMIP5 general circulation model (GCM)/regional climate model (RCM) couples from EURO-CORDEX (Jacob et al. 2014) under two emission scenarios (Representative Concentration Pathways, RCP 4.5 and RCP 8.5; see Table 1). A 30-year reference period in the past was selected, from 1970 to 1999, to compute anomalies and the prospective period covers the entire twenty-first century. We used daily outputs of downwelling solar radiation, 2-m air temperature, 10-m wind speed, precipitation, and relative humidity. All the outputs from the eight models were projected on a common regular grid over France with an 8-km spatial resolution, corresponding to the finest resolution of the RCMs. The use of two RCP scenarios makes it possible to assess the sensitivity of the results to the range of elevated atmospheric CO_2 concentration. Since RCM climate outputs are not unbiased, all results are shown as anomalies with respect to the 1970–1999 period, taken as the reference.

The evolution of CO_2 concentrations in atmospheric forcing CMIP5 projections is available online: http://www.pik-potsdam.de/~mmalte/rcps/ (Meinshausen et al. 2011). These projections report an increase of 185 ppm and 582 ppm, respectively, for RCP 4.5 and RCP 8.5, between 1991 and 2100.

2.2 Penman–Monteith PE formulation

We used the FAO56-PM equation (Allen et al. 1998):

$$\lambda \bullet PE = \frac{\Delta R_n + \left(\rho_a \bullet \frac{C_P}{r_a}\right)(e_s - e_a)}{\Delta + \gamma\left(1 + \frac{r_s}{r_a}\right)} \quad (1)$$

where Δ is the slope of saturation vapor pressure versus the air temperature curve (kPa $°C^{-1}$), γ is the psychrometric constant (kPa $°C^{-1}$), ρ_a is the air density (kg m^{-3}), C_P is the specific heat of air at constant pressure (J kg^{-1} $°C^{-1}$), e_s is the saturation vapor pressure (kPa) estimated from air temperature (°C) using the equation of Allen et al. (1998), e_a is the actual vapor pressure (kPa) derived from e_s (kPa) and relative humidity (in %), and λ is the latent heat of vaporization (J kg^{-1}) taken as a constant. Since not all GCM/RCM projections provided net radiation R_n (MJ m^{-2} day^{-1}) but instead downwelling shortwave and longwave solar radiation, net radiation was

Table 1 The eight CMIP5 GCM/RCM couples used in this study

General circulation model (GCM)	Regional climate model (RCM)
CNRM-CM5	CNRM-ALADIN63
CNRM-CM5	KNMI-RACMO22E
IPSL-CM5A-MR	SMHI-RCA4
MOHC-HadGEM2-ES	CLMcom-CCLM4-8–17
ICHEC-EC-EARTH	SMHI-RCA4
MPI-ESM-LR	CLMcom-CCLM4-8–17
MPI-ESM-LR	MPI-CSC-REMO2009
NCC-NorESM1-M	DMI-HIRHAM5

computed following the recommendations by Allen et al. (1998), using an albedo equal to 0.23 (-) and an upwelling longwave radiation as a function of emissivity and air temperature.

Assuming a grass reference surface of 0.12-m height, Allen et al. (1998) suggested an aerodynamic resistance r_a (s m^{-1}) inversely proportional to wind speed u (m s^{-1}) and a constant stomatal resistance $r_s = 70$ (s m^{-1}):

$$r_a = \frac{208}{u} \tag{2}$$

2.3 *Adjusting stomatal resistance with atmospheric CO_2 concentrations*

From compiling mostly experimental results, several authors proposed adjusting the stomatal resistance with respect to changes in atmospheric CO_2 concentrations. Allen (1990) proposed empirical adjustments of r_s for soybean, sweet corn, and sweetgum based on the experiments by Rogers et al. (1983). Stockle et al. (1992) suggested adjustments of r_s for different types of crops based on the experiments by Morison (1987). Kruijt et al. (2008) compiled several experimental studies to derive r_s adjustments for grass, wood crops, and C4 crops. From a different perspective, Yang et al. (2019) proposed a relationship between the change in r_s and the change in atmospheric CO_2 concentrations, so that the estimated AE from the Choudhury model fits the estimated AE simulated by several CMIP5 models under the RCP 8.5 scenario.

These proposed adaptations of r_s were all expressed as a fraction of a reference stomatal resistance r_{s_ref} at the atmospheric concentration of CO_2 equal to 330 ppm. The resulting functional relationships between stomatal resistance and atmospheric CO_2 are shown in Fig. 1.

In this paper, we did not consider the effect of plant species on r_s, and to remain consistent with PE usage in hydrological models, we retained only the equation proposed by Kruijt et al. (2008) corresponding to grass. Consequently, three functional relationships between relative change in r_s and atmospheric CO_2 concentration were used. The selection was made based on actual usage of these relationships for hydrological model applications.

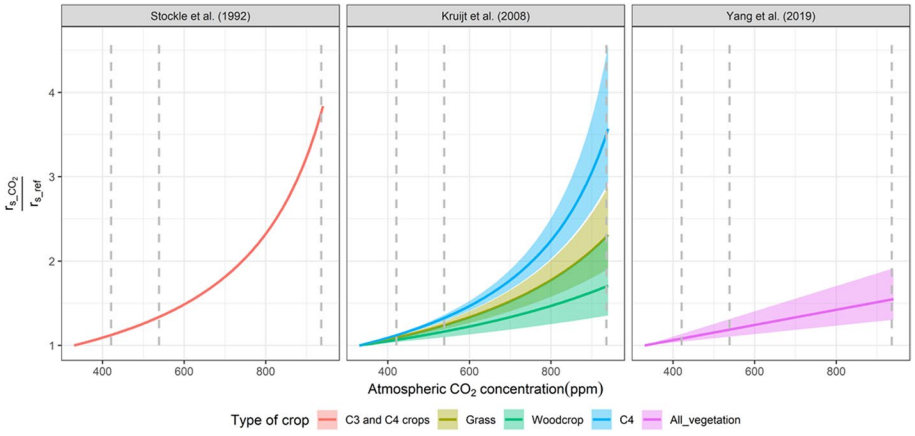

Fig. 1 Functional relationships between relative change in r_s and atmospheric CO_2 concentration. Uncertainty bounds are computed using the information from the original publications. Since Yang et al. (2019) did not explicitly take into consideration plant species, we retained the adaptations obtained from the mean climate model simulations and for the individual climate models representing the lower and upper bounds. The dashed vertical lines refer to the expected atmospheric CO_2 concentrations for 2100 under RCP 2.6 (left vertical line), RCP 4.5 (middle vertical line), and RCP 8.5 (right vertical line)

Table 2 presents the selected relationships, their acknowledged limits, and an inexhaustive list of some applications for hydrological modeling.

2.4 Budyko model

A change in PE does not necessarily lead to similar changes in runoff, due to the additional influence of soil moisture (Duethmann and Blöschl 2018). To account for these additional influences, we analyzed the evolution of annual runoff (Q) using the non-parametric Budyko (1974) equation:

$$Q = P - P\left[\frac{PE}{P} \bullet tanh\left(\frac{P}{PE}\right) \bullet \left(1 - e^{-\frac{PE}{P}}\right)\right]^{\frac{1}{2}} \quad (3)$$

with P the precipitation and all variables expressed in millimeter per year. The Budyko equation is one of the most widely used approaches to determine long-term AE. This equation is derived from long-term climate observations and highlights the connection of evapotranspiration with both precipitation and PE. With climate projections of both P and PE, this approach makes it possible to investigate the potential change in runoff under several climate projections. Thus, the Budyko framework has been used in climate impact studies at the national scale (Donohue et al. 2011; Renner and Bernhofer 2012; van der Velde et al. 2014). In this study, the Budyko equation is applied at the annual time scale, for each 8×8-km cell of the regular grid over France. This approach allows us to assess both (a) the temporal evolution of P, PE, and runoff over the entire domain and (b) the regional differences in these evolutions. While rather crude, the Budyko formulation appeared particularly able to simulate long-term runoff over some representative French catchments (see Supplementary Materials, Fig. S1).

3 Results

3.1 Changes in climate data and Budyko runoff induced by rising atmospheric CO_2

Precipitation anomalies are shown in Fig. 2 since they influence the simulated runoff in the Budyko equation. Precipitation trends are highly variable among RCMs, showing on average no trend under RCP 4.5 in the future relative to the reference period 1970–1999, and a slight decreasing trend by the end of the century under RCP 8.5 ($\Delta P = -22$ mm y^{-1}, corresponding to a relative decrease of −2%).

The impact of the choice of stomatal resistance on PE is evident for both RCP 4.5 and RCP 8.5 scenarios (Fig. 2). For RCP 4.5, the ensemble of climate models projects an increasing PE in the future relative to the reference period 1970–1999. All formulations that increase r_s with rising CO_2 lead to a lower PE increase compared to the reference Penman–Monteith formulation. The largest increase (ΔPE = +78 mm y^{-1} by the end of the century, corresponding to a relative increase of +11%) is obtained with the Penman–Monteith equation applied with constant r_s. Conversely, r_{s_Stockle} leads to a moderate increase (ΔPE is +33 mm y^{-1} by the end of the century, corresponding to a relative increase of +5%). For RCP 8.5, the evolutions in PE anomalies diverge and the trends depend greatly on the formulation of r_s chosen. The Penman–Monteith equation applied with constant r_s leads again to a more pronounced increase (ΔPE = +149 mm y^{-1}, corresponding to a relative increase of +21%). Conversely, the Penman–Monteith equation with modified r_{s_Stockle} leads to a decreasing PE at the end of the century (ΔPE = −20 mm y^{-1}, corresponding to a relative change of −3%), after a period of moderate increase until the 2070s. The two other formulations of r_s tested yield

Table 2 Functional relationships used in this study to assess the impact of CO_2. $r_{s\_Stockle}$ r_{s_Kruijt}, and r_{s_Yang} refer to the modified stomatal resistances taking into account elevated atmospheric CO_2; r_{s_ref} is the reference stomatal resistance taken in this study at 70 s m.$^{-1}$; and CO_{2ref} is the reference concentration of atmospheric CO_2, taken at 330 ppm in this study

Original reference	Notation	Equation used in this study	Comments	Previous hydrological applications
Stockle et al. (1992)	$r_{s_}$Stockle	$\frac{r_{s\_\text{Stockle}}}{r_{s\_ref}} = \frac{1}{1.4-0.4\frac{CO_2}{CO_{2\,\text{ref}}}}$	Derived from experimental results for C3 and C4 crops. The range of applicability is up to 660 ppm	Mainly SWAT model applications (Wu et al. 2012; Butcher et al. 2014; Kim et al. 2017)
Kruijt et al. (2008)	$r_{s_}$Kruijt	$\frac{r_{s\_\text{Kruijt}}}{r_{s\_ref}} = \frac{1}{1-9.3\bullet10^{-4}(CO_2-CO_{2\,\text{ref}})}$	Derived from experimental results for three types of crops, the equation used here is for grass. The range of applicability is up to 660 ppm	Some national case studies with diverse rainfall–runoff models (Kruijt et al. 2008; Rasmussen et al. 2012; Rudd and Kay 2015; Guillod et al. 2018)
Yang et al. (2019)	$r_{s_}$Yang	$\frac{r_{s\_\text{Yang}}}{r_{s\_ref}} = 1 + 9 \bullet 10^{-4}\left(CO_2 - CO_{2\,\text{ref}}\right)$	Derived by fitting the AE simulated by the Choudhury model to the AE simulated by climate model	Yang et al. 2019

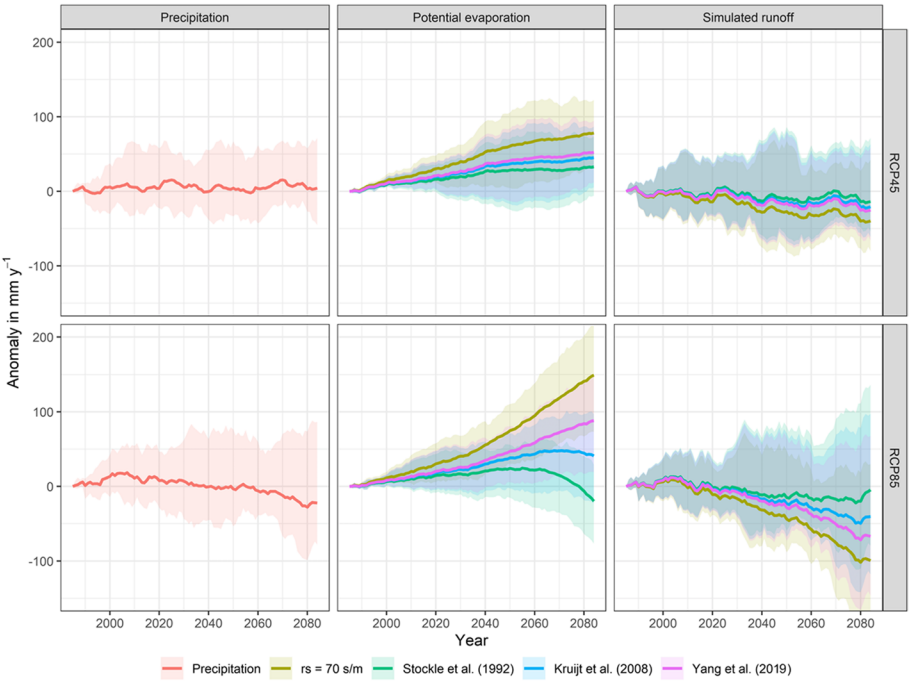

Fig. 2 Evolution of precipitation (left), PE (middle), and simulated runoff using the Budyko equation (right) relative to the 1970–1999 period for the RCP 4.5 and RCP 8.5 scenarios, averaged over France. The colored shadings represent the min–max estimation range from to climate models and the solid lines represent the mean. Data are smoothed with a 30-year running mean. Detailed values are given in Appendix

intermediate positive changes. The increase in PE is more pronounced from RCP 4.5 to RCP 8.5 using r_{s_Yang}, while r_{s_Kruijt} yields a lower increase under the RCP 8.5 scenario, showing that the increase in PE due to enhanced vapor pressure deficit is offset by the increase in stomatal resistance due to rising CO_2. The PE uncertainties due to RCM projections generally increase during the period. Under the RCP 4.5 scenario, the uncertainties in PE due to climate projections are comparable to the uncertainties in PE due to the r_s formulation, while PE uncertainties due to the r_s formulation are larger under RCP 8.5.

The implications of these different PE evolutions for simulated runoff are evident although dependent also on precipitation evolution (Fig. 2). For the RCP 4.5 scenario, the ensemble of climate models projects a limited decrease in simulated runoff in the future relative to the reference period 1970–1999 (ΔQ ranges from -40 mm y^{-1} to -14 mm y^{-1} by the end of the century, corresponding to relative changes of -6% to -2%, respectively). For the RCP 8.5 scenario, runoff anomaly evolutions are globally negative but diverge more among PE formulations. The Penman–Monteith equation applied with constant r_s leads to the most pronounced decrease ($\Delta Q = -99$ mm y^{-1} by the end of the century, corresponding to a relative decrease of -14%), while Penman–Monteith r_{s_Stockle} leads to a very slight decrease ($\Delta Q = -4$ mm y^{-1}, corresponding to a relative change of -1%). There is a large variability among climate model simulations and some climate models project positive runoff changes for both RCP 4.5 and RCP 8.5, whatever the r_s formulation used.

3.2 Spatial patterns of changes

There is a meridional gradient for precipitation changes over France, with negative and positive trends in the southern and northern parts, respectively (Fig. 3). This gradient is more important for RCP 8.5 than for RCP 4.5. The magnitude of differences between the selected adaptations of stomatal resistance is in agreement with the time series presented in Fig. 2. Under RCP 8.5, r_{s_Stockle} and r_{s_Kruijt} formulations produce a decreasing PE (up to − 15%) in some regions, particularly over the northwestern coast. For these regions, positive trends in precipitation and negative trends in PE suggest larger spatial discrepancies in the simulated runoff. For RCP 4.5, for the reference formulation and r_{s_Yang}, an increase in PE is projected over the whole territory.

Spatial patterns of simulated runoff changes vary dramatically across the selected formulations of stomatal resistance (Fig. 4). The decrease is general using the Penman–Monteith equation applied with constant r_s, with southern regions experiencing a decrease that can reach − 50%. The adaptations of the stomatal resistance provide a more nuanced picture, with a decrease in runoff in southern areas and an increase in runoff in the northern areas, up to + 30%. These uncertainties in the sign of runoff changes are also evident across climate projections, since climate model trends agree only in limited areas, whatever the PE formulation selected (Fig. 5). Only for RCP 8.5 and southern France is there agreement between the eight models on a decreased runoff.

3.3 Comparison with actual evapotranspiration and runoff as estimated by RCMs

PE projections are compared to actual evapotranspiration derived from RCMs for non-water-stressed grid cells (i.e., PE/P < 0.75 during both historical and future periods), where PE and AE (actual evapotranspiration) are likely close. The results are presented in Fig. 6, in which we compare the average evolution of PE and AE over the twenty-first century for both RCP 4.5 and RCP 8.5. The RCMs show on average a small increase in AE, even in "energy-limited" regions, while the PE projections with a reference formulation (r_s set at 70 m s^{-1}) predict a

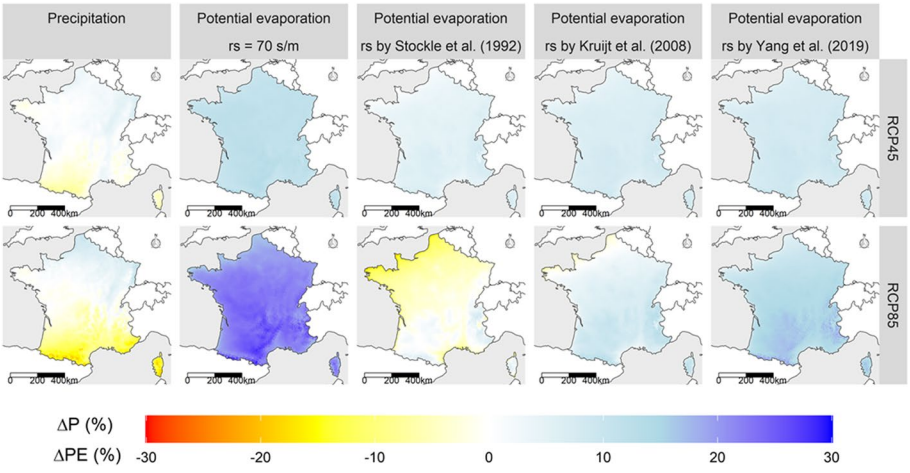

Fig. 3 Ensemble mean of relative annual precipitation and PE changes (%) between the 1970–1999 and 2070–2099 periods under the RCP 4.5 and RCP 8.5 scenarios with different formulations of stomatal resistance

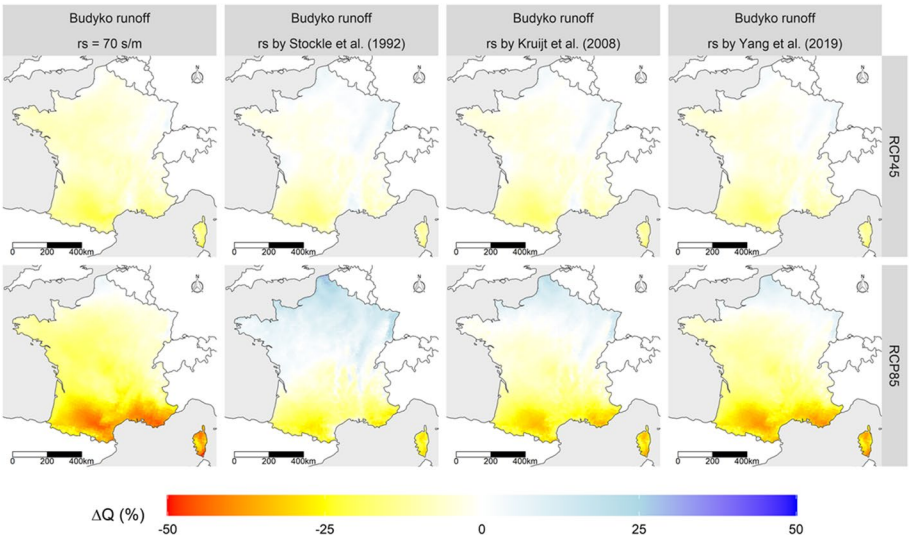

Fig. 4 Ensemble mean of relative annual simulated runoff changes (%) using the Budyko equation between the 1970–1999 and 2070–2099 periods under the RCP 4.5 and RCP 8.5 scenarios with different formulations of stomatal resistance

very large increase. However, the formulations taking into account atmospheric CO_2 (with modified r_s) seem to better fit the RCMs' AE. Nevertheless, the r_{s_Stockle} formulation projects a decrease in PE after 2070, which is inconsistent with AE trend estimated by the RCMs. The same observation can be made for r_{s_Kruijt} at the long lead-time.

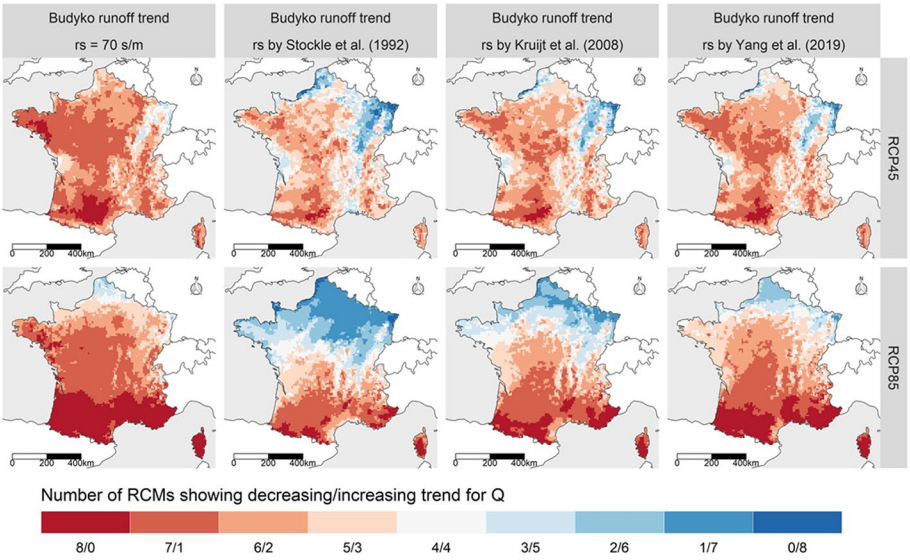

Fig. 5 Partition of the number of RCMs (out of 8) showing decreasing/increasing runoff using the Budyko equation between the 1970–1999 and 2070–2099 periods under the RCP 4.5 and RCP 8.5 scenarios with different formulations of stomatal resistance

The runoff averaged over France as simulated by RCMs (taken as precipitation minus AE) presents relatively similar trends to those obtained with the Budyko equation (Fig. 7). For the RCP 4.5 scenario, the runoff decreases slightly over time, in general agreement with the runoff estimated under the Budyko framework with the different PE formulations. For the RCP 8.5 scenario, runoff anomalies from RCMs are globally negative (except for Stockle's formulation) but less pronounced than those estimated under the Budyko framework. The mean of the RCM ensemble leads to a very slight decrease ($\Delta Q = -31$ mm y^{-1}), a value that lies between the runoff simulated with r_{s_Kruijt} ($\Delta Q = -40$ mm y^{-1}) and the one obtained with r_{s_Stockle} ($\Delta Q = -4$ mm y^{-1}). The simulated runoff from the Penman–Monteith equation applied with constant r_s leads to a clearly more important decrease that is close to the minimum of the runoff estimates.

The spatial patterns of changes in runoff (Fig. 6) corroborate these findings: for both RCP 4.5 and RCP 8.5, the spatial patterns of change given by the RCMs are close to those obtained using r_{s_Stockle} and r_{s_Kruijt}, i.e., a distinct trend between northern and southern regions.

4 Discussion

4.1 Comparing changes with previous model experiments

The Budyko equation used in this study to simulate runoff is relatively straightforward and neglects key processes such as the seasonality of P and PE. Besides, the climate projections from RCMs used in this paper were not bias-corrected. Thus, we did not intend to produce reliable estimates of the impact of climate, but rather to investigate the spectrum of changes

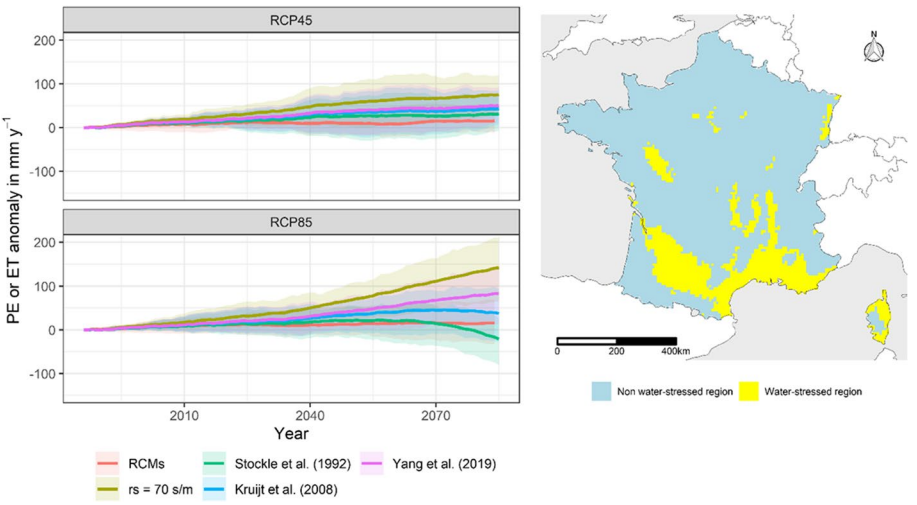

Fig. 6 Left: Evolution of simulated PE and RCM-AE relative to the 1970–1999 period for the RCP 4.5 and RCP 8.5 scenarios. The colored shadings represent the min–max estimation range in AE and PE estimations and the solid lines represent the mean. Data are smoothed with a 30-year running mean. Right: In blue, the non-water stressed grid cells selected over the study area, with a threshold criterion (PE/P) < 0.75, over historical and future periods; in yellow, water-limited regions over France that were not *selected for the comparison*

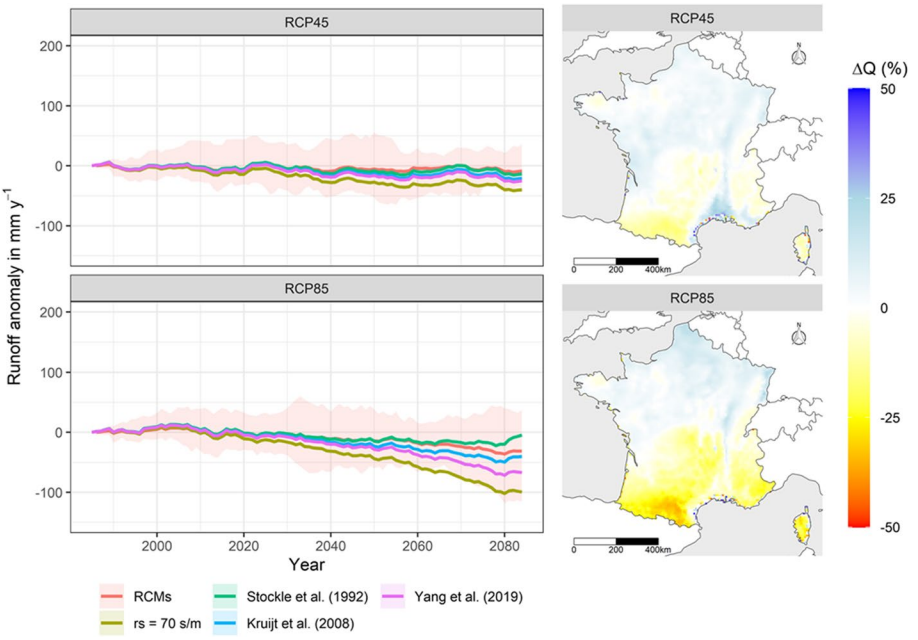

Fig. 7 Left: Evolution of simulated runoff using the RCM simulations relative to the 1970–1999 period for the RCP 4.5 and RCP 8.5 scenarios. The colored shadings represent the min–max estimation range in RCM runoff estimation and the solid lines represent the mean. Data are smoothed with a 30-year running mean. Right: Ensemble mean of relative annual RCM simulated runoff changes (%) between the 1970–1999 and 2070–2099 periods under the RCP 4.5 and RCP 8.5 scenarios

associated with the choice of a formulation of PE that takes into account the influence of CO_2 on stomatal resistance. The regional pattern changes in annual runoff obtained in this study are, however, in agreement with previous studies (Donnelly et al. 2017; Dayon et al. 2018) that used more complex hydrological models: a pronounced decline in mean runoff in the southern part of France, no clear runoff changes in the northern part of France, with large uncertainties stemming from climate projections. We also showed that these patterns are in general agreement with RCM outputs, which means that despite the simplicity of the Budyko equation, it enables us to reproduce the simulation of more physically based coupled climate models.

Perspectives of using r_s formulations accounting for CO_2 in PE formulations in future studies.

As expected, taking into account the influence of CO_2 on r_s limits both PE and AE, and thus also limits the decline in runoff, particularly in energy-limited regions. The choice of the formulation of r_s is therefore significant for studies on the impact of climate change on runoff. The three formulations tested in this paper provide quite different runoff projections compared with the classic use of the Penman–Monteith equation with constant r_s. The differences are obvious under the RCP 8.5 but also present under the RCP 4.5 scenario. It is noteworthy that the different trends (and sign of the trend) are highly variable compared to differences of changes in PE when considering different PE formulations (Lemaitre-Basset et al. 2021), showing that the uncertainties in projections of CO_2 concentrations might be translated to large uncertainties in PE (and simulated runoff).

While the use of the Budyko framework highlights moderate-to-important impacts of taking into account CO_2 in PE formulations, how this could reflect on hydrological projections made with rainfall–runoff hydrological models might not be straightforward. The impact of PE formulations on discharge projections is still under debate, some studies pointing to either a low impact (Dakhlaoui et al. 2020) or a high impact (Seiller and Anctil 2016). Specifically, the presence of a parameter calibration in most hydrological models might distort the relationship between PE anomalies and runoff anomalies (Oudin et al. 2006) and could lead to different results from those simulated with the Budyko framework.

4.2 *Limitations of taking into account CO_2 in PE formulations*

While there are many good reasons for adjusting r_s with CO_2, the choice of a single formulation is complicated. Two existing formulations, namely, the formulations by Stockle et al. (1992) and by Kruijt et al. (2008), were developed from experimental results for selected types of crops, and their range of applicability is up to 660 ppm, i.e., far below the expected CO_2 content by the end of century under the RCP 8.5 scenario (935 ppm in 2100). Indeed, increasing stomatal resistance indefinitely is not realistic, as plants must continue to ensure gas exchange, even with a highly enriched CO_2 atmosphere. Thus, the use of these empirical formulations for the RCP 8.5 scenario is as questionable as the use of these formulations for large-scale applications with mixed land use. The third formulation, proposed by Yang et al. (2019), was derived by fitting the AE simulated by the Choudhury model to the AE simulated by climate models, the rationale being that climate models allow us to take into account surface–atmosphere interactions more explicitly. This formulation was calibrated at the global scale and we showed that it probably needs some regional adjustments, since the runoff simulated using this formulation is not fully in line with RCM outputs over France.

The fertilization effect of atmospheric CO_2 on the growth of plants may produce an opposite effect by promoting both PE and AE. Nevertheless, this theory is in fact limited in the context of long-term exposure (climate change): Ainsworth and Rogers (2007) showed a reduction in photosynthesis activity, called "down-regulation," and a slowdown of the greening trend on many biomes was pointed out by Winkler et al. (2021). Besides, plant growth needs fertilizers (e.g., nitrogen), and their availability in the environment will limit the fertilization effect of CO_2, thus reducing the CO_2 sink role of terrestrial vegetation (Wang et al. 2020). This competing effect of CO_2 on AE can theoretically be taken into account in r_s formulations through the use of the leaf area index (LAI). However, determining LAI in the future requires a dynamic vegetation model and presents relatively high uncertainties (Yang et al. 2019). Over France, simulated LAI with different GCMs generally shows a positive trend (between 0.05% y^{-1} in the south and 0.1% y^{-1} in the north). Since the formulation proposed by Yang et al. (2019) was derived by minimizing the discrepancies between AE simulated by Budyko and GCMs, it implicitly takes into account the positive role of LAI. This may explain the lower effect of CO_2 on stomatal resistance compared with Stockle et al. (1992) and Kruijt et al. (2008).

The use of simple functional relationships between r_s and CO_2 for correcting PE estimates may be seen as "flogging a dead horse." Translating complex surface–atmosphere feedbacks into a simple adjustment of the PE equation neglects several other possible effects, and it is still uncertain how AE will evolve under climate change. For example,

Xiao et al. (2020) showed that AE tends to decline under climate change, owing to decreased relative humidity and consequent stomatal closure due to the decreased moisture gradient at the leaf surface. Nevertheless, for most PE formulations, the opposite occurred, since reducing relative humidity increases PE. In the same time, Dong and Dai (2017) showed diverging results, with increases in AE in the past decades, associated with an important uncertainty. Finally, some studies show a plausible trend in AE without representing soil and vegetation effects, but using a parameterized relationship with observed data.

5 Conclusion

In this study, we assessed the impact of taking into account CO_2 in the Penman–Monteith PE formulation. We showed that taking into account CO_2 in this PE formulation leads to reduced PE amounts. On the basis of the Budyko framework, we have shown that the inclusion of CO_2 in PE formulations limits the annual runoff reduction, especially in an emissive scenario, namely, the RCP 8.5 scenario, and even increases annual runoff in some regions, whereas the classic Penman–Monteith formulation leads to decreasing runoff projections over most of France, taking into account CO_2 leads to more contrasting results, with runoff increase that becomes likely in the north of France, which is an energy-limited area. However, the three formulations tested involve different shades of runoff response. The results suggest that climate change impact studies that use PE formulations that do not make use of CO_2 may underestimate runoff under a future climate. However, uncertainty remains in the way CO_2 can be included in PE formulations, as can be seen from the three options tested here, which questions the intensity of hydrological projection changes due to the inclusion of CO_2.

The common way to compute PE for hydrological models in climate impact studies ignores the negative feedback from terrestrial vegetation on AE. To correct the bias between PE evolution and AE in climate impact studies, we recommend estimating PE with an adjusted Penman–Monteith formulation, or another form (e.g., Peiris and Döll 2021). The formulation proposed by Yang et al. (2019) shows good potential for adjusting PE with respect to CO_2 concentrations; nevertheless, the relationship should be recalibrated with respect to the study region. On the other hand, the models proposed by Stockle et al. (1992) and Kruijt et al. (2008) show good agreement with the moderate emission scenario RCP 4.5, which is encouraging. However, these models were developed with atmospheric CO_2 concentrations limited to 660 ppm, which is much lower than the concentrations of the high emission scenario by the end of the twenty-first century. Probably due to extrapolation of the equation of r_s with CO_2 for these models above 660 ppm, PE estimates with these formulations lead to decreasing trends of PE by the end of century, which is not consistent with AE trends produced by RCMs. Finally, further observations are needed to include the effect of vegetation feedback on PE more precisely, including the evolution of vegetation yield through, e.g., simulated evolution of leaf area index, and limitation of the air vapor pressure deficit. The compensation between LAI and stomatal closure may depend on the type of environment (dry, wet, forest, crop field, grassland, etc.), which limits the generalization of our results to similar environments. Therefore, our conclusions show that the way PE formulations account for CO_2 is a lead for a possible improvement of eco-hydrological impact studies.

Appendix Detailed P, PE, and runoff values depending on RCP and formulation of r_s

Table 3 Values of P, PE, and simulated runoff using the Budyko equation for two climate periods (1970–1999 and 2070–2099) depending on the choice of r_s and the RCP. The mean value over the 8 GCMs/RCMs is indicated along with the min–max range

Variable	Historical	RCP 4.5			RCP 8.5		
	Period (1970–1999) in mm y^{-1}	Period (2070–2099) in mm y^{-1}	Anomaly in mm y^{-1}	Anomaly in percentage	Period (2070–2099) in mm y^{-1}	Anomaly in mm y^{-1}	Anomaly in percentage
Precipitation	1191 [811, 1421]	1195 [802, 1459]	4 [−45, 71]	0 [−4, 6]	1169 [762, 1413]	−22 [−78, 87]	−2 [−7, 7]
Potential evapotranspiration with r_{s_ref}	686 [613, 765]	765 [664, 887]	78 [36, 123]	11 [5, 16]	836 [732, 979]	149 [74, 215]	21 [11, 28]
Potential evapotranspiration with $r_{s\_Stockle}$	683 [610, 762]	716 [621, 834]	33 [−6, 73]	5 [−1, 10]	664 [576, 790]	−20 [−77, 29]	−3 [−11, 4]
Potential evapotranspiration with r_{s_Kruijt}	684 [611, 762]	729 [632, 848]	45 [6, 87]	6 [1, 11]	725 [632, 858]	41 [−23, 97]	6 [−3, 13]
Potential evapotranspiration with $r_{s_{Yang}}$	680 [607, 758]	733 [635, 852]	53 [12, 95]	8 [2, 13]	768 [671, 905]	88 [19, 148]	13 [3, 20]
Simulated runoff with r_{s_ref}	789 [383, 1032]	749 [328, 1002]	−40 [−80, 42]	−6 [−14, 5]	690 [271, 906]	−99 [−180, 30]	−14 [−29, 4]
Simulated runoff with $r_{s\_Stockle}$	791 [384, 1034]	777 [346, 1031]	−14 [−54, 72]	−2 [−10, 9]	786 [331, 1011]	−4 [−79, 136]	−1 [−14, 16]
Simulated runoff with r_{s_Kruijt}	790 [384, 1033]	769 [341, 1023]	−21 [−61, 64]	−3 [−11, 8]	750 [307, 971]	−40 [−118, 97]	−6 [−20, 12]
Simulated runoff with $r_{s_{Yang}}$	793 [386, 1036]	768 [340, 1021]	−25 [−66, 59]	−4 [−12, 7]	726 [292, 945]	−67 [−147, 68]	−10 [−24, 8]

Supplementary Information The online version contains supplementary material available at https://doi.org/10.1007/s10584-022-03384-1.

Acknowledgements The authors acknowledge Météo-France for preparing the EURO-CORDEX climate projections. The first author was funded by Sorbonne University and by Agence de l'Eau Rhin-Meuse.

Author contribution TLB, LO, and GT conceived the experimental set up and performed the calculation. All authors contributed to the final version of the manuscript.

Funding The Agence de lEau Rhin-Meuse contribute to funds this publication, grant no. AID-2020–00972.

Data availability The PE formulation codes used to account for the effect of CO_2 on stomatal resistance can be retrieved from http://doi.org/10.15454/NCNCHG.

Declarations

Ethics approval Not applicable.

Consent to participate Not applicable.

Consent for publication Not applicable.

Competing interests The authors declare no competing interests.

References

Addor N, Rössler O, Köplin N et al (2014) Robust changes and sources of uncertainty in the projected hydrological regimes of Swiss catchments. Water Resour Res 50:7541–7562. https://doi.org/10.1002/2014WR015549

Ainsworth EA, Rogers A (2007) The response of photosynthesis and stomatal conductance to rising [CO_2]: mechanisms and environmental interactions: photosynthesis and stomatal conductance responses to rising [CO_2]. Plant Cell Environ 30:258–270. https://doi.org/10.1111/j.1365-3040.2007.01641.x

Allen LH (1990) Plant responses to rising carbon dioxide and potential interactions with air pollutants. J Environ Qual 19:15–34. https://doi.org/10.2134/jeq1990.00472425001900010002x

Allen LH (1991) 7. Effects of increasing carbon dioxide levels and climate change on plant growth, evapotranspiration, and water resources. In: Managing water resources in the west under conditions of climate uncertainty: a proceedings. National Academies Press, Washington. https://doi.org/10.17226/1911

Allen RG, Pereira L, Raes D, Smith M (1998) Crop evapotranspiration: guidelines for computing crop water requirements. FAO Drainage and Irrigation Paper 56. Food and Agriculture Organization, Rome

Bosmans JHC, van Beek LPH, Sutanudjaja EH, Bierkens MFP (2017) Hydrological impacts of global land cover change and human water use. Hydrol Earth Syst Sci 21:5603–5626. https://doi.org/10.5194/hess-21-5603-2017

Budyko MI (1974) Climate and life, English ed édition (David H. Miller, Translator). Academic Press, New York

Bunce JA (2004) Carbon dioxide effects on stomatal responses to the environment and water use by crops under field conditions. Oecologia 140:1–10. https://doi.org/10.1007/s00442-003-1401-6

Butcher JB, Johnson TE, Nover D, Sarkar S (2014) Incorporating the effects of increased atmospheric CO_2 in watershed model projections of climate change impacts. J Hydrol 513:322–334. https://doi.org/10.1016/j.jhydrol.2014.03.073

Cheng L, Zhang L, Wang Y-P et al (2014) Impacts of elevated CO2, climate change and their interactions on water budgets in four different catchments in Australia. J Hydrol 519:1350–1361. https://doi.org/10.1016/j.jhydrol.2014.09.020

Chiew FHS, Teng J, Vaze J, Post DA, Perraud JM, Kirono DGC, Viney NR (2009) Estimating climate change impact on runoff across southeast Australia: method, results, and implications of the modeling method. Water Resour Res 45. https://doi.org/10.1029/2008WR007338

Dakhlaoui H, Seibert J, Hakala K (2020) Sensitivity of discharge projections to potential evapotranspiration estimation in Northern Tunisia. Reg Environ Change 20:34. https://doi.org/10.1007/s10113-020-01615-8

Dayon G, Boé J, Martin E, Gailhard J (2018) Impacts of climate change on the hydrological cycle over France and associated uncertainties. Comptes Rendus Geosci 350:.https://doi.org/10.1016/j.crte.2018.03.001

Dong B, Dai A (2017) The uncertainties and causes of the recent changes in global evapotranspiration from 1982 to 2010. Clim Dyn 49:279–296. https://doi.org/10.1007/s00382-016-3342-x

Donnelly C, Greuell W, Andersson J et al (2017) Impacts of climate change on European hydrology at 1.5, 2 and 3 degrees mean global warming above preindustrial level. Clim Change 143:13–26. https://doi.org/10.1007/s10584-017-1971-7

Donohue RJ, Roderick ML, McVicar TR (2011) Assessing the differences in sensitivities of runoff to changes in climatic conditions across a large basin. J Hydrol 406:234–244. https://doi.org/10.1016/j.jhydrol.2011.07.003

Duethmann D, Blöschl G (2018) Why has catchment evaporation increased in the past 40 years? A data-based study in Austria. Hydrol Earth Syst Sci 22:5143–5158. https://doi.org/10.5194/hess-22-5143-2018

Forzieri G, Feyen L, Rojas R et al (2014) Ensemble projections of future streamflow droughts in Europe. Hydrol Earth Syst Sci 18:85–108. https://doi.org/10.5194/hess-18-85-2014

Gedney N, Cox PM, Betts RA et al (2006) Detection of a direct carbon dioxide effect in continental river runoff records. Nature 439:835–838. https://doi.org/10.1038/nature04504

Gerten D, UK RB, Döll P (2014) 2014: cross-chapter box on the active role of vegetation in altering water flows under climate change. In: Field CB, Barros VR, Dokken DJ, Mach KJ, Mastrandrea MD, Bilir TE, Chatterjee M, Ebi KL, Estrada YO, Genova RC, Girma B, Kissel ES, Levy AN, MacCracken S, Mastrandrea PR, White LL (eds) Climate change 2014: impacts, adaptation, and vulnerability. Part A: global and sectoral aspects. Contribution of Working Group II to the Fifth Assessment Report of the Intergovernmental Panel on Climate Change. Cambridge University Press, Cambridge and New York, pp 157–161

Guillod BP, Jones RG, Dadson SJ et al (2018) A large set of potential past, present and future hydro-meteorological time series for the UK. Hydrol Earth Syst Sci 22:611–634. https://doi.org/10.5194/hess-22-611-2018

Hakala K, Addor N, Teutschbein C et al (2019) Hydrological modeling of climate change impacts. In: Encyclopedia of water. American Cancer Society, pp 1–20. https://doi.org/10.1002/9781119300762.wsts0062

Inauen N, Körner C, Hiltbrunner E (2013) Hydrological consequences of declining land use and elevated CO_2 in alpine grassland. J Ecol 101:86–96. https://doi.org/10.1111/1365-2745.12029

Islam A, Ahuja LR, Garcia LA et al (2012) Modeling the effect of elevated CO2 and climate change on reference evapotranspiration in the semi-arid Central Great Plains. Trans ASABE 55:2135–2146. https://doi.org/10.13031/2013.42505

Jacob D, Petersen J, Eggert B et al (2014) EURO-CORDEX: new high-resolution climate change projections for European impact research. Reg Environ Change 14:563–578. https://doi.org/10.1007/s10113-013-0499-2

Kim Y, Band LE, Ficklin DL (2017) Projected hydrological changes in the North Carolina piedmont using bias-corrected North American Regional Climate Change Assessment Program (NARCCAP) data. J Hydrol Reg Stud 12:273–288. https://doi.org/10.1016/j.ejrh.2017.06.005

Kruijt B, Witte J-PM, Jacobs CMJ, Kroon T (2008) Effects of rising atmospheric CO_2 on evapotranspiration and soil moisture: a practical approach for the Netherlands. J Hydrol 349:257–267. https://doi.org/10.1016/j.jhydrol.2007.10.052

Kumar S, Zwiers F, Dirmeyer PA et al (2016) Terrestrial contribution to the heterogeneity in hydrological changes under global warming. Water Resour Res 52:3127–3142. https://doi.org/10.1002/2016WR018607

Lemaitre-Basset T, Oudin L, Thirel G, Collet L (2021) Unravelling the contribution of potential evaporation formulation to uncertainty under climate change. Hydrol Earth SystSci Discuss 1–18. https://doi.org/10.5194/hess-2021-361

Le Quéré C, Moriarty R, Andrew RM et al (2015) Global carbon budget 2015. Earth Syst Sci Data 7:349–396. https://doi.org/10.5194/essd-7-349-2015
Ma N, Zhang Y (2022) Increasing Tibetan Plateau terrestrial evapotranspiration primarily driven by precipitation. Agric for Meteorol 317:108887. https://doi.org/10.1016/j.agrformet.2022.108887
Ma N, Szilagyi J, Jozsa J (2020) Benchmarking large-scale evapotranspiration estimates: a perspective from a calibration-free complementary relationship approach and FLUXCOM. J Hydrol 590:125221. https://doi.org/10.1016/j.jhydrol.2020.125221
Ma N, Szilagyi J, Zhang Y (2021) Calibration-free complementary relationship estimates terrestrial evapotranspiration globally. Water Resour Res 57. https://doi.org/10.1029/2021WR029691
Meinshausen M, Smith SJ, Calvin K et al (2011) The RCP greenhouse gas concentrations and their extensions from 1765 to 2300. Clim Change 109:213–241. https://doi.org/10.1007/s10584-011-0156-z
Milly PCD, Dunne KA (2016) Potential evapotranspiration and continental drying. Nat Clim Change 6:946–949. https://doi.org/10.1038/nclimate3046
Morison JIL (1987) Intercellular CO2 concentration and stomatal response to CO_2. In: Zeiger E (ed) Stomatal function. G.D.Farquhar & I.R. Cowan. Stanford University Press, Stanford, pp 229–252
Naumann G, Alfieri L, Wyser K et al (2018) Global changes in drought conditions under different levels of warming. Geophys Res Lett 45:3285–3296. https://doi.org/10.1002/2017GL076521
Oudin L, Perrin C, Mathevet T et al (2006) Impact of biased and randomly corrupted inputs on the efficiency and the parameters of watershed models. J Hydrol 320:62–83. https://doi.org/10.1016/j.jhydrol.2005.07.016
Pan S, Tian H, Dangal SRS et al (2015) Responses of global terrestrial evapotranspiration to climate change and increasing atmospheric CO_2 in the 21st century. Earths Future 3:15–35. https://doi.org/10.1002/2014EF000263
Peiris TA, Döll P (2021) A simple approach to mimic the effect of active vegetation in hydrological models to better estimate hydrological variables under climate change, EGU General Assembly 2021, online, 19–30 Apr 2021, EGU21-12025, 10.5194/egusphere-egu21-12025
Prudhomme C, Giuntoli I, Robinson EL et al (2014) Hydrological droughts in the 21st century, hotspots and uncertainties from a global multimodel ensemble experiment. Proc Natl Acad Sci 111:3262–3267. https://doi.org/10.1073/pnas.1222473110
Rasmussen J, Sonnenborg TO, Stisen S et al (2012) Climate change effects on irrigation demands and minimum stream discharge: impact of bias-correction method. Hydrol Earth Syst Sci 16:4675–4691. https://doi.org/10.5194/hess-16-4675-2012
Renner M, Bernhofer C (2012) Applying simple water-energy balance frameworks to predict the climate sensitivity of streamflow over the continental United States. Hydrol Earth Syst Sci 16:2531–2546. https://doi.org/10.5194/hess-16-2531-2012
Rogers HH, Bingham GE, Cure JD et al (1983) Responses of selected plant species to elevated carbon dioxide in the field. J Environ Qual 12:569–574. https://doi.org/10.2134/jeq1983.00472425001200040028x
Rosenberg NJ, McKenney MS, Martin P (1989) Evapotranspiration in a greenhouse-warmed world: a review and a simulation. Agric for Meteorol 47:303–320. https://doi.org/10.1016/0168-1923(89)90102-0
Roudier P, Andersson J, Donnelly C et al (2016) Projections of future floods and hydrological droughts in Europe under a +2°C global warming. Clim Change 135. https://doi.org/10.1007/s10584-015-1570-4
Rudd AC, Kay AL (2015) Use of very high resolution climate model data for hydrological modelling: estimation of potential evaporation. Hydrol Res 47:660–670. https://doi.org/10.2166/nh.2015.028
Scheff J, Frierson DMW (2014) Scaling potential evapotranspiration with greenhouse warming. J Clim 27:1539–1558. https://doi.org/10.1175/JCLI-D-13-00233.1
Seiller G, Anctil F (2016) How do potential evapotranspiration formulas influence hydrological projections? Hydrol Sci J 61:2249–2266. https://doi.org/10.1080/02626667.2015.1100302
Stockle CO, Williams JR, Rosenberg NJ, Jones CA (1992) A method for estimating the direct and climatic effects of rising atmospheric carbon dioxide on growth and yield of crops: Part I–modification of the EPIC model for climate change analysis. Agric Syst 38:225–238
van der Velde Y, Vercauteren N, Jaramillo F et al (2014) Exploring hydroclimatic change disparity via the Budyko framework. Hydrol Process 28:4110–4118. https://doi.org/10.1002/hyp.9949
Wada Y, Wisser D, Eisner S et al (2013) Multimodel projections and uncertainties of irrigation water demand under climate change. Geophys Res Lett 40:4626–4632. https://doi.org/10.1002/grl.50686
Wang S, Zhang Y, Ju W et al (2020) Recent global decline of CO_2 fertilization effects on vegetation photosynthesis. Science 370:1295–1300. https://doi.org/10.1126/science.abb7772
Winkler AJ, Myneni RB, Hannart A et al (2021) Slowdown of the greening trend in natural vegetation with further rise in atmospheric CO_2. Biogeosciences 18:4985–5010. https://doi.org/10.5194/bg-18-4985-2021

Wu Y, Liu S, Abdul-Aziz O (2012) Hydrological effects of the increased CO2 and climate change in the Upper Mississippi River Basin using a modified SWAT. Clim Change 110:977–1003. https://doi.org/10.1007/s10584-011-0087-8

Xiao M, Yu Z, Kong D et al (2020) Stomatal response to decreased relative humidity constrains the acceleration of terrestrial evapotranspiration. Environ Res Lett 15:094066. https://doi.org/10.1088/1748-9326/ab9967

Yang Y, Roderick ML, Zhang S et al (2019) Hydrologic implications of vegetation response to elevated CO_2 in climate projections. Nat Clim Change 9:44–48. https://doi.org/10.1038/s41558-018-0361-0

Yin J, He F, Xiong YJ, Qiu GY (2017) Effects of land use/land cover and climate changes on surface runoff in a semi-humid and semi-arid transition zone in northwest China. Hydrol Earth Syst Sci 21:183–196. https://doi.org/10.5194/hess-21-183-2017